RSC Publishing Faraday Discussions

Model Potential Study of Non-valence Correlation-bound Anions of $(C_{60})_n$ Clusters: the Role of Electric Field-Induced Charge Transfer

Journal:	*Faraday Discussions*
Manuscript ID	FD-ART-11-2018-000199
Article Type:	Paper
Date Submitted by the Author:	21-Nov-2018
Complete List of Authors:	Choi, Tae Hoon; University of Pittsburgh, Department of Chemistry Jordan, Kenneth; University of Pittsburgh, Department of Chemistry

Faraday Discussions

ARTICLE

Model Potential Study of Non-Valence Correlation-Bound Anions of $(C_{60})_n$ Clusters: the Role of Electric Field-Induced Charge Transfer

Received 00th January 20xx,
Accepted 00th January 20xx

DOI: 10.1039/x0xx00000x

www.rsc.org/

Tae Hoon Choi and Kenneth D. Jordan*

A polarization model which accounts for electric field-induced charge transfer between fullerene molecules is introduced. Application of this model to the C_{60} dimer and trimer shows that intermolecular charge transfer makes a significant contribution to the polarizabilities of these clusters. This polarization model is incorporated into a one-electron Hamiltonian for describing non-valence correlation-bound anions, allowing us to further demonstrate that intermolecular charge transfer also results in increased stability of these anion states.

1. Introduction

Sufficiently polarizable molecules (or clusters) can form non-valence correlation-bound (NVCB) anions in which the excess electron is bound in a diffuse non-valence orbital, with electron correlation being essential for the stability of the ion.[1-7] The theoretical treatment of NVCB anions using *ab initio* methods is especially challenging since it is necessary to employ a method for including correlation effects that does not depend on the suitability of the Hartree-Fock (HF) wave function as the starting point and to use flexible basis sets with multiple sets of diffuse functions. In fact, with the flexible basis sets required to describe NVCB anions, HF calculations on the excess electron system collapse onto the neutral plus a discretized continuum orbital. As a result, methods such as second-order Møller-Plesset perturbation theory (MP2)[8] and even coupled cluster with single and double and perturbative triple excitations [CCSD(T)] ,[9] when starting from the HF wave function, can fail to bind the excess electron. The equation-of-motion coupled cluster singles and doubles (EOM-CCSD) method[10] has proven to be one of the most successful *ab initio* methods for characterizing NVCB anions.

An alternative approach for describing non-valence anions is to employ a model Hamiltonian in which only the excess electron is treated explicitly.[7, 11-13] In a recent study, our group introduced a one-electron model Hamiltonian (hereafter referred to as the VJ model) for describing NVCB anions of fullerenes.[7] The development of this model was motivated by experimental measurements indicating the existence of NVCB anions of C_{60} molecules adsorbed on the Cu (110) surface.[14, 15] In the VJ model, the electron-molecule potential is expressed as

$$V = V^{es} + V^{pol} + V^{rep}, \quad (1)$$

where V^{es}, V^{pol}, V^{rep} are electrostatic, polarization, and repulsion terms, respectively. The correlation effects essential for the electron binding in a many-electron treatment are incorporated through the V^{pol} term. Long-range electrostatics (i.e., contributions outside the overlap region) are relatively unimportant for the NVCB anion states of fullerenes, and in the VJ model this contribution is effectively described through the use of atomic dipoles on the C atoms. V^{pol}, which is described in detail below, allows for atom-centered induced dipoles as well as for a charge-flow polarization.[16] V^{rep}, which consists of a single Gaussian centered on each atom, absorbs the effects of charge penetration, exchange, and orthogonalization. The parameters in V^{rep} were chosen so that the electron binding energy (EBE) and charge distribution of the excess electron of the NVCB anion of C_{60} as described by the model potential closely match the corresponding quantities from large-basis set EOM-CCSD calculations.[6]

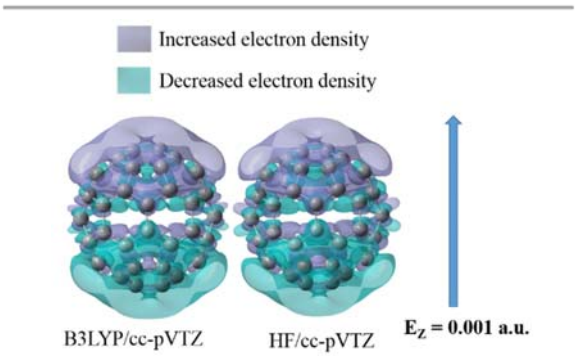

Fig. 1 The change in the charge distribution of C_{60} resulting from the application of a uniform electric field of 0.001 a.u. along the z axis. Isovalues are ±0.00003e/a.u.^{3}.

Department of Chemistry, University of Pittsburgh, Pittsburgh, Pennsylvania, 15260, United States
E-mail: Jordan@pitt.edu
Electronic Supplementary Information (ESI) available: See DOI:

The motivation for the use of a polarization model allowing for charge-flow polarization is provided by Fig. 1 which depicts the change in the charge distribution of C_{60} resulting from the application of a uniform electric field of 0.001 a.u. The charge density difference was calculated using the B3LYP density functional method[17-20] in conjunction with the cc-pVTZ basis set.[21] As seen from the figure, the external field induces a significant displacement of charge from one side of the molecule to the other. A similar change in the charge distribution is obtained in the HF approximation, thus the finding of a sizable field-induced intramolecular charge transfer is not an artifact of the DFT method. These calculations and the B3LYP and HF calculations described below were carried out using the Gaussian 16 program.[22]

The polarization contribution to the energy for an isolated fullerene molecule was described using a model introduced by Mayer and Åstrand[23]:

$$E_{pol} = \frac{1}{2}\sum_{i=1}^{N}\sum_{j=1}^{N} q_i T_{q-q}^{ij} q_j - \frac{1}{2}\sum_{i=1}^{N}\sum_{j=1}^{N} \mathbf{p}_i \cdot \mathbf{T}_{p-p}^{ij} \cdot \mathbf{p}_j - \sum_{i=1}^{N}\sum_{j=1}^{N} \mathbf{p}_i \cdot \mathbf{T}_{p-q}^{ij} q_j + \sum_{i=1}^{N} q_i V_i - \sum_{i=1}^{N} \mathbf{p}_i \cdot \mathbf{E}_i \qquad (2)$$

where q_i and $\mathbf{p}_i$ refer to the induced charge and dipole moment at site i, and V_i and $\mathbf{E}_i$ are the external potential and electric field at site i. When using eqn (2) in modeling an excess electron interacting with a molecule or cluster, V_i and $\mathbf{E}_i$ derive from the excess electron. In order to determine the values of the charges and induced dipoles from eqn (2), one adds a charge-conservation term via a Lagrange multiplier, and then minimizes the polarization energy with respect to the q_i and $\mathbf{p}_i$.

If one applies eqn (2) to clusters by treating the entire system as a supermolecule, one encounters the problem that the amount of charge transferred between molecules increases with their separation, which is an unphysical result. Recognizing this, in the earlier application of the VJ model Hamiltonian approach to characterize the NVCB anions of $(C_{60})_2$, charge transfer between the molecules was not allowed.[7] In the present study, we extend the Mayer-Åstrand polarization model to provide a more physically correct description of charge transfer between molecules, and use the modified model to calculate the dipole polarizabilities and electron binding energies (EBEs) of the NVCB anions of the $(C_{60})_n$, n = 2 and 3, clusters.

In the remainder of this manuscript we refer to the model not allowing intermolecular charge transfer as the Mayer-Åstrand model, and that which treats the cluster as a supermolecue as the "supermolecule Mayer-Åstrand model". Finally we refer to our modified Mayer-Åstrand model, described below, as an "extended Mayer-Åstrand model".

2. Methodology

In a quantum mechanical treatment, starting from a wave function of the form $\mathcal{A}\psi_A\psi_B$, where ψ_A and ψ_B are Hartree-Fock wave functions of molecules A and B, respectively, and $\mathcal{A}$ antisymmetrizes electrons between the two molecules, the field-induced charge transfer between the two molecules can be expressed as a sum of terms involving the overlap of occupied orbitals on one monomer with the unfilled orbitals on the other. Thus one would expect the charge-transfer to fall off exponentially with increasing separation between the molecules. That this is indeed the case is seen from Fig. 2 which reports the charge transfer calculated at the B3LYP/cc-pVTZ level between two C_{60} molecules with their centers on the *z*-axis and an electric field of 0.001 a.u. in the *z*-direction. The net charge on each molecule was determined using the Mulliken procedure.[24] Similar values for the intermolecular charge transfer are obtained using the Hirschfeld procedure.[25] At the minimum energy separation (center-to-center) between the molecules (R = 9.75 Å)[26] the B3LYP calculations predict that a charge of 0.013 |e| is transferred from one C_{60} molecule to the other due to the presence of the applied electric field. At R = 9.0 Å, which corresponds approximately to the point on the repulsive wall of the intermolecular potential where the interaction energy is zero, the net charge transfer is 0.06 |e|.

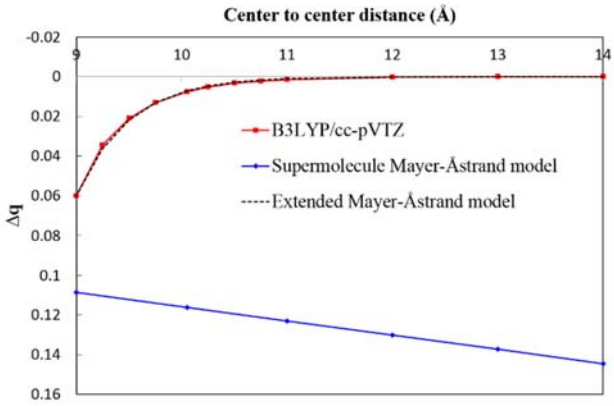

Fig. 2 Electric field-induced charge transfer between two C_{60} molecules as a function of their center-to-center distance. Results are reported from electric field of 0.001 a.u. in the z-direction

As seen from Fig. 2, the charge transfer obtained from the supermolecule Mayer-Åstrand model grows linearly with increasing separation between the monomers. In extending the Mayer-Åstrand model to include intermolecular charge transfer in a physically correct manner, we introduce a single exponential damping factor depending on the center-to-center separations of the fullerene molecules as described in the ESI.† In spite of the simplicity of this approach, it accurately reproduces the electric field-induced charge transfer determined from the B3LYP calculations as shown in Fig. 2. In assessing the performance of the extended Mayer-Åstrand model for predicting the polarizabilities of the C_{60} dimer and trimer, comparison is made with the results of B3LYP calculations carried out using the cc-pVTZ and cc-pVQZ(*-f,-g*)

Table 1 Polarizabilities (Å^3) of the C_{60} monomer and the C_{60} dimer at R = 9.50, 9.75, and 10.05 Å

Method	C_{60}	$(C_{60})_2$					
		R= 9.50 Å		R= 9.75 Å		R= 10.05 Å	
	$\alpha_{xx}=\alpha_{yy}=\alpha_{zz}$	$\alpha_{xx}=\alpha_{yy}$	α_{zz}	$\alpha_{xx}=\alpha_{yy}$	α_{zz}	$\alpha_{xx}=\alpha_{yy}$	α_{zz}
B3LYP/cc-pVTZ	78	144	223	145	209	146	198
B3LYP/cc-pVQZ(*-f, -g*)	82	149	229	150	215	151	204
Model without intermolecular CT[a]	76	140	199	142	188	142	183
Model with intermolecular CT[a]	76	140	238	142	216	142	200

[a]CT denotes charge transfer

basis sets,[21] where the (*-f,-g*) indicates that the *f* and *g* functions were omitted from the basis set.

The energies and orbitals associated with the NVCB anions of C_{60} and its dimer and trimer as described by the model Hamiltonians were calculated using a grid-based discrete variable representation (DVR) approach[27] as implemented in the PISCES code.[28] In the model Hamiltonian, described in detail in Ref. 7, the excess electron interacts with permanent dipoles as well as induced dipoles and induced charges on each C atom. We refer to the model Hamiltonian based on the extended Mayer-Åstrand polarization model as the extended VJ model.

3. Results and Discussion

3.1 C_{60} monomer and dimer

For the C_{60} monomer the Mayer-Åstrand model gives a polarizability of 76 Å^3 which is essentially identical to the experimental value of 76.5 Å^3.[29] B3LYP calculations with the cc-pVTZ and cc-pVQZ*(-g,-f)* basis sets give slightly larger polarizability values of 78 and 82 Å^3, respectively. Table 1 reports for $(C_{60})_2$ at R = 9.50, 9.75, and 10.05 Å, the polarizabilities obtained from B3LYP calculations, from the Mayer-Åstrand model with no charge transfer between the monomers, and from the extended model allowing for intermonomer charge transfer. For the range of distances considered, the values of α_{xx} and α_{yy} (which are equal due to symmetry) from the B3LYP calculations and from the two polarization models are quite close and 7−10% smaller than twice the polarizability of the monomer. In contrast, the α_{zz} component grows significantly when the separation between the two molecules is decreased from 10.05 to 9.50 Å. Also, the α_{zz} values calculated using the model allowing for intermolecular charge transfer closely reproduce the α_{zz} values from the B3LYP calculations, while the model neglecting this contribution underestimates α_{zz}, with the extent of underestimation growing with decreasing R.

The net polarizability from the model potential calculations has three contributions: that due to the atom-centered induced dipoles, that due to charge-transfer (both intra- and inter-monomer), and that due to the coupling of the point-induced dipoles and the charge-flow terms. The first two contributions are positive, while the coupling term makes a negative contribution. As seen from Table 2, the net polarizability of C_{60} has contributions of 158 and 192 Å^3 from the point inducible dipoles and the charge flow, respectively. These contributions are significantly attenuated by the cross term of -274 Å^3 between the induced dipoles and charge flow contributions, with the net polarizability being only 76 Å^3. If the charge transfer contribution is removed from the energy expression, the polarizability from the induced dipoles is calculated to be only 60 Å^3. For the dimer, the contributions to the polarizability from the induced dipoles and from the coupling term undergo little change when R is decreased from 10.05 to 9.50 Å (and are approximately twice the corresponding values of the monomer), and the increase in α_{zz} with decreasing R is almost entirely a consequence of intermonomer charge transfer.

Fig. 3 reports for the C_{60} dimer with 9.50 Å separation the change in the charge distribution of the caused by an electric

Table 2 Polarizability contributions (Å^3) to C_{60} and $(C_{60})_2$, at R = 9.50, 9.75, and 10.05 Å, calculated using the extended Mayer-Åstrand model.

Contri-bution	Compo-nent	C_{60}	$(C_{60})_2$		
			R = 9.50 Å	R = 9.75 Å	R = 10.05 Å
Induced dipole	$\alpha_{xx}=\alpha_{yy}$	158.0	314.3	315.0	315.1
	α_{zz}	158.0	320.0	318.9	318.5
charge-flow	$\alpha_{xx}=\alpha_{yy}$	192.0	376.8	378.0	378.5
	α_{zz}	192.0	457.1	434.9	419.4
cross term	$\alpha_{xx}=\alpha_{yy}$	−273.7	−551.0	−551.3	−551.3
	α_{zz}	−273.7	−538.8	−538.3	−537.8
Total	$\alpha_{xx}=\alpha_{yy}$	76.2	140.1	141.6	142.4
	α_{zz}	76.2	238.4	215.5	200.0

Table 3 Electron binding energies (meV) of the NVCB anions of $(C_{60})_2$ at R = 9.50, 9.75, and 10.05 Å

Sym-metry	R = 9.50 Å		R = 9.75 Å		R = 10.05 Å	
	without CT[a]	with CT[a]	without CT[a]	with CT[a]	without CT[a]	with CT[a]
σ_g	244	263	250	263	253	261
σ_u	104	126	98	112	96	105
π_u	65	76	62	69	59	63
σ_g	0	4	2	7	5	8

[a] CT denotes charge transfer

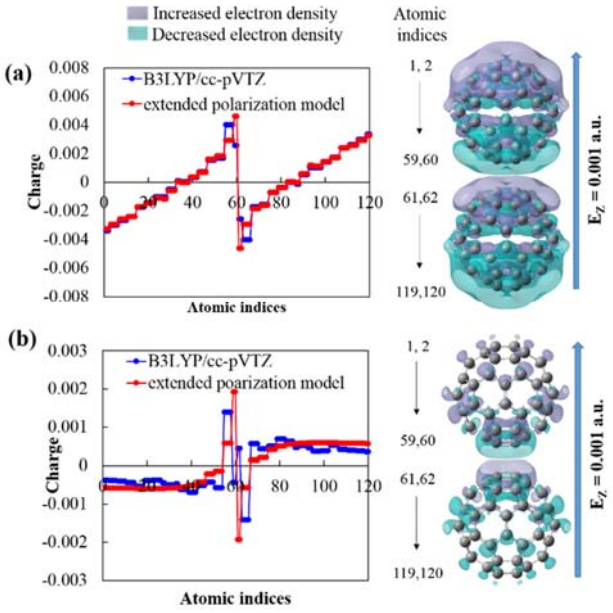

Fig. 3 The changes in the atomic charges and the charge distribution of the C_{60} dimer with 9.5 Å separation caused by an electric field of 0.001 a.u. along the z axis. (a) The left-hand side shows changes in the atomic charges from B3LYP calculations and from the extended Mayer-Åstrand model. The right-hand side shows the field-induced changes in the charge density at the B3LYP/cc-pVTZ level. (b) Same as (a) except that the field-induced changes in the charge (left) and charge distributions (right) of the non-interacting monomers are subtracted from those shown in (a). Isovalues for the charge density differences are ±0.00003e/a.u.^{3}. The atoms are numbered starting from the top of the upper molecule to the bottom of the lower molecule.

field of 0.001 a.u. along the *z* axis. Results are reported for both B3LYP/cc-pVTZ calculations and for the extended Mayer-Åstrand model. The charge distribution changes are analyzed in two different ways. The right-hand side of Fig. 3a plots the difference of the B3LYP/cc-pVTZ charge densities of the dimer calculated with and without the electric field. The left-hand side of this figure reports the associated changes in the atomic charges from Mulliken analysis of the B3LYP charge distribution and from the extended Mayer-Åstrand model. From Fig. 3a it is seen that, except for the atoms of the two molecules that are closest to one another, the extended Mayer-Åstrand model and the B3LYP calculations yield very similar changes in the charges as a result of the application of the electric field. In Fig. 3b, the charge density differences are corrected to remove the field-induced changes in the non-interacting monomers. The right-hand side of this figure reports the quantity

$$\Delta\rho = \rho_{(\text{dimer with field})} - \rho_{(\text{dimer without field})} - \rho_{(\text{monomer with field})} + \rho_{(\text{monomer without field})} \quad (3)$$

where ρ is the charge density. The associated changes in the atomic charges are reported in the left-hand side of Fig. 3b. The results reported in Fig. 3b show that the charge rearrangements of the "contact" atoms of the two molecules are in the direction opposite that of the net charge transfer, and that it is the changes in the charges of the more distant atoms that is responsible for the intermolecular charge transfer in the expected direction. From the left-hand side of Fig. 3b, it can be seen that roughly the same charge is transferred from all non-contact C atoms of one C_{60} molecule to the non-contact C atoms of the other C_{60} molecule.

We now examine the impact of electric field-induced charge transfer on the EBEs of the NVCB anions of the C_{60} dimer, reporting results obtained from the model potential with and without inclusion of intermolecular charge transfer. The results of these calculations at dimer separations of 9.50, 9.75 and 10.0 Å are reported in Table 3. Over this range of distances, the calculations locate four NVCB anion states, two of Σ_g symmetry, and one each of Π_u and Σ_u symmetry, with the second Σ_g anion state being only marginally bound. At R = 9.75 Å, the calculations with the extended VJ model give EBEs of 263, 112, and 69 meV for the lowest energy Σ_g, Π_u, and Σ_u NVCB anion states, respectively. These should be compared to the 130 meV EBE calculated using the VJ model for the A_g NVCB anion of C_{60}. As expected, the EBEs of the various NVCB anion states are enhanced by the inclusion of intermonomer charge transfer, with the enhancement growing with decreasing separation between the two C_{60} molecules.

3.2 C_{60} trimer

Both linear and equilateral triangular structures were considered for $(C_{60})_3$. The structures of the C_{60} trimers were

Table 4 Polarizabilities (Å^3) of the linear and equilateral triangular C_{60} trimer at R = 9.50, 9.75, and 10.05 Å

Molecule	Method	R = 9.50 Å		R = 9.75 Å		R = 10.05 Å	
		α_{xx} (α_{yy})	α_{zz}	α_{xx} (α_{yy})	α_{zz}	α_{xx} (α_{yy})	α_{zz}
$(C_{60})_3$ linear	B3LYP/cc-pVTZ	210	394	211	357	213	330
	B3LYP/cc-pVQZ(-*f*, -*g*)	217	403	218	366	220	339
	Model without intermolecular CT[a]	205	322	206	310	208	299
	Model with intermolecular CT[a]	205	437	206	378	208	339
$(C_{60})_3$ triangular	B3LYP/cc-pVTZ	311 (301)	202	294 (287)	204	279 (274)	205
	B3LYP/cc-pVQZ(-*f*, -*g*)	319 (309)	209	302 (294)	210	287 (282)	212
	Model without intermolecular CT[a]	262	197	258	199	254	201
	Model with intermolecular CT[a]	312	197	291	199	275	201

[a]CT denotes charge transfer

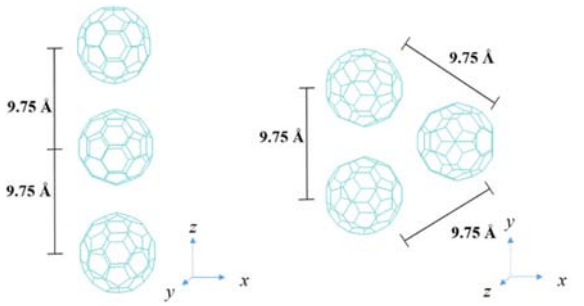

Fig. 4 The geometries of linear and triangular $(C_{60})_3$ with 9.75 Å separation.

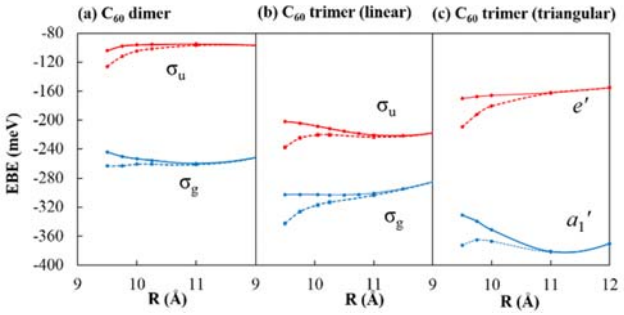

Fig. 5 The energies of the two most stable NVCB anion states for (a) $(C_{60})_2$ (b) linear $(C_{60})_3$, and (c) equilateral triangular $(C_{60})_3$ as a function of the intermonomer distances. Results are reported for the VJ model (solid line) and the extended VJ model allowing for intermolecular charge transfer (dashed line).

generated by adding a monomer to the C_{60} dimer oriented along the *z* direction as shown in Fig. 4. The dipole polarizabilities of the two forms of the C_{60} trimer with intermonomer separations of 9.50, 9.75 and 10.05 Å are reported in Table 4. Comparison of the results obtained from B3LYP calculations for the linear trimer with those for the dimer reveals that the α_{zz} component of the polarizability grows more rapidly with decreasing *R* for the trimer than for the dimer. Comparison of the results of the calculations with the Mayer-Åstrand and extended Mayer-Åstrand models reveals that this is a consequence of intermolecular charge transfer. Qualitatively, this can be understood in terms of the larger separation of the transferred charge in the linear trimer than in the dimer with equivalent intermonomer separations.

Intermolecular charge transfer is also found to be important for the in-plane polarization of the equilateral triangular C_{60} trimer. Although the changes in α_{xx} and α_{yy} of the equilateral trimer due to the inclusion of intermolecular charge transfer are only about half as large as that in α_{zz} of the linear trimer, the charge transfer contributions are approximately the same for the average polarizability $\alpha = 1/3(\alpha_{xx} + \alpha_{yy} + \alpha_{zz})$, of the two structures. Table 5 reports the contributions of the induced point dipoles, the charge-flow, and the coupling term to the net polarizabilities of the $(C_{60})_3$ clusters. As was found for the dimer, the strongest distance dependence is displayed by the charge-flow contribution.

Table 6 reports the EBEs of the linear and equilateral triangular forms of $(C_{60})_3$ for intermonomer separations of 9.50, 9.75, and 10.05 Å. Five NVCB anions, two of Σ_g symmetry, two of Σ_u symmetry, and one of Π_u symmetry, are predicted for the linear trimer. The binding energies of all five anions are enhanced by the inclusion of intermolecular charge transfer in the polarization model, with the percentage enhancement being smallest for the most strongly bound anion and growing in importance as one progresses to more weakly bound anion states, being 43% for the second Σ_u anion at *R* = 9.75 Å. The model Hamiltonian calculations also give five NVCB anions for the equilateral triangular form of the C_{60} trimer. Two are of A_1' symmetry, two of E' symmetry, and one of A_2'' symmetry. As for the linear form of the trimer the inclusion of electric field-induced intermolecular charge transfer is most important for the NVBC anions with the smallest EBEs, with the percentages increases for the second A_1' and second E' anion states being 47 and 112%, respectively.

Fig. 5 reports the energies of the two most stable NVCB anion states of $(C_{60})_2$ and of the two structures for $(C_{60})_3$ for separations ranging from 9.50 to 12 Å. For each of the three systems, it is seen that the intermolecular charge transfer contribution to the EBE ceases to be important for separations

Table 5 Polarizability contributions (Å³) calculated using the extended Mayer-Åstrand model for $(C_{60})_3$ at *R* = 9.50, 9.75, and 10.05 Å

Contribution	Component	$(C_{60})_3$ linear			$(C_{60})_3$ triangular		
		R = 9.50 Å	*R* = 9.75 Å	*R* = 10.05 Å	*R* = 9.50 Å	*R* = 9.75 Å	*R* = 10.05 Å
Induced dipole	$\alpha_{xx} = \alpha_{yy}$	471.4	471.9	472.1	477.4	476.7	476.2
	α_{zz}	481.6	480.5	479.5	470.7	471.2	471.6
charge-flow	$\alpha_{xx} = \alpha_{yy}$	562.3	563.4	564.7	657.7	632.0	614.3
	α_{zz}	754.6	693.9	656.4	558.4	559.7	561.0
cross term	$\alpha_{xx} = \alpha_{yy}$	−829.0	−829.2	−829.1	−823.1	−818.1	−815.8
	α_{zz}	−798.7	−796.3	−797.1	−832.1	−832.2	−831.9
Total	$\alpha_{xx} = \alpha_{yy}$	204.7	206.1	207.8	312.0	290.5	274.7
	α_{zz}	437.5	378.1	338.8	197.0	198.8	200.7

Table 6 Electron binding energies (meV) of the NVCB anions of $(C_{60})_3$.

	Symmetry	*R* = 9.50 Å		*R* = 9.75 Å		*R* = 10.05 Å	
		without CT[a]	with CT[a]	without CT	with CT[a]	without CT	with CT[a]
$(C_{60})_3$ linear	σ_g	303	342	302	326	303	317
	σ_u	202	237	204	225	208	220
	π_u	109	134	104	118	98	106
	σ_g	79	112	77	96	76	88
	σ_u	15	36	14	20	14	22
$(C_{60})_3$ triangular	a_1'	331	372	339	365	351	367
	e'	170	209	167	192	166	180
	a_2''	156	182	152	168	147	157
	a_1'	24	48	32	47	42	52
	e'	16	46	16	34	16	27

[a] CT denotes charge transfer

greater than 11 Å. Fig. 6 plots for each of the three clusters considered the enhancement of the EBE of the most stable NVCB anion vs. the enhancement of the polarizability resulting from the inclusion of intermolecular charge transfer. For the two structures considered for the trimer there is a near linear relation between these two quantities, with approximately the same slope for the two isomers. For small polarizability enhancements the corresponding curve for the dimer closely follows those of the trimers, but for larger polarizability enhancements, the curve for the dimer deviates from linear.

Fig. 7 depicts the orbitals occupied by the excess electron in the NVCB anion states of the C_{60} dimer and the linear C_{60} trimer at an intermonomer separation of 9.75 Å. As noted above, for the C_{60} molecule the only stable NVCB anion is the *s*-like A_g state with the *p*-like NVCB anion being slightly unbound (i.e., metastable). Were the NVCB anion states of $(C_{60})_2$ and linear $(C_{60})_3$ derived solely from linear combinations of the *s*-like NVCB anion state for C_{60}, one would expect to see a single bound (Σ_g) NVCB anion of $(C_{60})_2$ and two (Σ_g and Σ_u) NVCB anions of linear $(C_{60})_3$. Both the dimer and trimer display more NVCB anions than this due to the states derived from the metastable *p*-like non-valence anion state of C_{60} and due to *sp* hybridization. We note also that if we use the EBEs of the π_u NVCB anions of $(C_{60})_2$ and linear $(C_{60})_3$ to determine α and β parameters for a Huckel model for the π-type NVCB orbitals, this simple analysis predicts the *p*-type NVCB anion of C_{60} to be unbound by ~50 meV, consistent with our model potential calculations that predict it to be unbound.

The orbitals associated with the NVCB anion states of the triangular C_{60} trimer are shown in Fig. 8. The most stable NVCB orbital of a_1' symmetry for the equilateral trimer is dominated by the bonding combination of the *s*-type NVCB anion orbitals of C_{60}. However, the *e'* orbitals associated with the next most stable NVCB anion display considerable *sp* hybridization and, as

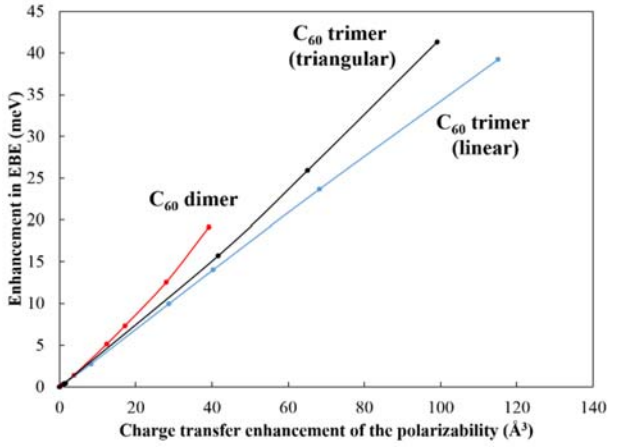

Fig. 6 Relation between the enhancement of the EBE of the most stable NVCB anions of $(C_{60})_2$ and the linear and triangular forms of $(C_{60})_3$, and the enhancement in the polarizability as a result of inclusion of intermolecular charge transfer. The values on the horizontal axis are α_{zz} for $(C_{60})_2$ and linear $(C_{60})_3$ and $\alpha_{xx} + \alpha_{yy}$ for triangular $(C_{60})_3$.

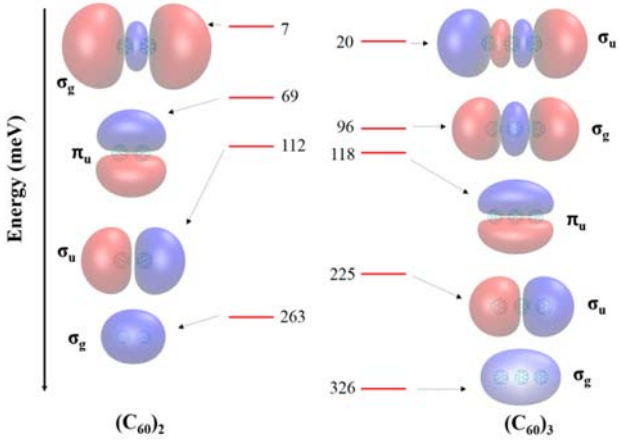

Fig. 7 Orbitals associated with the NVCB anion states of the C_{60} dimer and the linear C_{60} trimer at an intermonomer separation of 9.75 Å. The orbital isosurfaces enclose 90% of the charge of the excess electron.

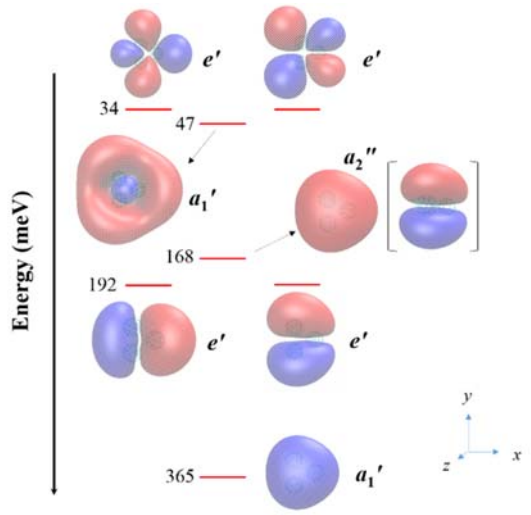

Fig. 8 Orbitals associated with the various NVCB anion states of the equilateral triangular C_{60} trimer at an intermonomer separation of 9.75 Å. The orbital isosurfaces enclose 90% of the charge of the excess electron.

a result, are more stable than were only the *s*-type orbital associated with the A_g NVCB anion of the C_{60} monomers involved. The energy of the a_2'' π-like NVCB anion orbital of the equilateral trimer falls energetically close to where one would expect based on the location of the *p*-type non-valence anion of C_{60} and the π_u NVCB anion of $(C_{60})_2$. The second a_1' NVCB orbital of $(C_{60})_3$ is essentially a bonding combination of the *p*-type NVCB anion of the C_{60} monomers. The second degenerate *e*' NVCB anion orbital of the equilateral trimer also derives from a combination of the *p*-type NVCB orbitals of the monomers.

4. Conclusions

In this study the polarizability model of Ref. 23 is extended to account for electric field-induced intermolecular charge transfer in C_{60} clusters. This extended polarization model was incorporated in a model Hamiltonian for describing non-valence correlation-bound anions. It is found that, at the potential energy minimum of the C_{60} dimer, the inclusion of the charge transfer term leads to a 15% increase in the α_{zz} value of the dimer. For the C_{60} trimer, the contribution of intermolecular charge-flow to the average polarizabilities is even more important. This increase of the polarizabilities is accompanied by a 5–15% increase in the EBEs of the low-energy NVCB anion states of the C_{60} dimer and trimer. The inclusion of intermolecular charge transfer is found to be even more important for excited NVCB anion states with small EBEs.

Conflicts of interest

There are no conflicts to declare.

Acknowledgements

This research was supported by the National Science Foundation under grant CHE1762337. The calculations were carried out on computers in the University of Pittsburgh's Center for Research Computing.

References

1. V. K. Voora, A. Kairalapova, T. Sommerfeld and K. D. Jordan, *J. Chem. Phys.*, 2017, **147**, 214114.
2. S. Klaiman, E. V. Gromov and L. S. Cederbaum, *Phys. Chem. Chem. Phys.*, 2014, **16**, 13287-13293.
3. T. Sommerfeld, *J. Chem. Theory Comput.*, 2013, **9**, 4866-4873.
4. V. K. Voora and K. D. Jordan, *J. Phys. Chem. A*, 2014, **118**, 7201-7205.
5. J. P. Rogers, C. S. Anstöter and J. R. R. Verlet, *J. Phys. Chem. Lett.*, 2018, **9**, 2504-2509.
6. V. K. Voora, L. S. Cederbaum and K. D. Jordan, *J. Phys. Chem. Lett.*, 2013, **4**, 849-853.
7. V. K. Voora and K. D. Jordan, *Nano Lett.*, 2014, **14**, 4602-4606.
8. C. Møller and M. S. Plesset, *Phys. Rev.*, 1934, **46**, 618-622.
9. J. A. Pople, M. Head-Gordon and K. Raghavachari, *J. Chem. Phys.*, 1987, **87**, 5968-5975.
10. J. F. Stanton and R. J. Bartlett, *J. Chem. Phys.*, 1993, **98**, 7029-7039.
11. V. K. Voora, J. Ding, T. Sommerfeld and K. D. Jordan, *J. Phys. Chem. B*, 2013, **117**, 4365-4370.
12. L. Turi and D. Borgis, *J. Chem. Phys.*, 2002, **117**, 6186-6195.
13. L. D. Jacobson and J. M. Herbert, *J. Chem. Phys.*, 2010, **133**, 154506.
14. M. Feng, J. Zhao and H. Petek, *Science*, 2008, **320**, 359-362.
15. M. Feng, J. Zhao, T. Huang, X. Zhu and H. Petek, *Acc. Chem. Res.*, 2011, **44**, 360-368.
16. A. Stone, *The Theory of Intermolecular Forces, 2nd ed*, Oxford, 2013.
17. S. H. Vosko, L. Wilk and M. Nusair, *Can. J. Phys.*, 1980, **58**, 1200-1211.
18. C. Lee, W. Yang and R. G. Parr, *Phys. Rev. B*, 1988, **37**, 785-789.
19. A. D. Becke, *J. Chem. Phys.*, 1993, **98**, 5648-5652.
20. P. J. Stephens, F. J. Devlin, C. F. Chabalowski and M. J. Frisch, *J. Phys. Chem.*, 1994, **98**, 11623-11627.
21. T. H. Dunning Jr, *J. Chem. Phys.*, 1989, **90**, 1007-1023.
22. Gaussian 16, Revision B.01, M. J. Frisch, G. W. Trucks, H. B. Schlegel, G. E. Scuseria, M. A. Robb, J. R. Cheeseman, G. Scalmani, V. Barone, G. A. Petersson, H. Nakatsuji, X. Li, M. Caricato, A. V. Marenich, J. Bloino, B. G. Janesko, R. Gomperts, B. Mennucci, H. P. Hratchian, J. V. Ortiz, A. F. Izmaylov, J. L. Sonnenberg, Williams, F. Ding, F. Lipparini, F. Egidi, J. Goings, B. Peng, A. Petrone, T. Henderson, D. Ranasinghe, V. G. Zakrzewski, J. Gao, N. Rega, G. Zheng, W. Liang, M. Hada, M. Ehara, K. Toyota, R. Fukuda, J. Hasegawa, M. Ishida, T. Nakajima, Y. Honda, O. Kitao, H. Nakai, T. Vreven, K. Throssell, J. A. Montgomery Jr., J. E. Peralta, F. Ogliaro, M. J. Bearpark, J. J. Heyd, E. N. Brothers, K. N. Kudin, V. N. Staroverov, T. A. Keith, R. Kobayashi, J. Normand, K. Raghavachari, A. P. Rendell, J. C. Burant, S. S. Iyengar, J. Tomasi, M. Cossi, J. M. Millam, M. Klene, C.

Adamo, R. Cammi, J. W. Ochterski, R. L. Martin, K. Morokuma, O. Farkas, J. B. Foresman and D. J. Fox, *Gaussian, Inc., Wallingford CT,* 2016.
23. A. Mayer and P. O. Åstrand, *J. Phys. Chem. A*, 2008, **112**, 1277-1285.
24. R. S. Mulliken, *J. Chem. Phys.*, 1962, **36**, 2306.
25. F. L. Hirshfeld, *Theor. Chim. Acta*, 1977, **44**, 129.
26. D. I. Sharapa, J. T. Margraf, A. Hesselmann and T. Clark, *J. Chem. Theory Comput.*, 2017, **13**, 274-285.
27. T. H. Choi, T. Sommerfeld, S. L. Yilmaz and K. D. Jordan, *J. Chem. Theory Comput.*, 2010, **6**, 2388-2394.
28. T. Sommerfeld, T.-H. Choi, V. K. Voora and K. D. Jordan, *Pittsburgh InfraStructure for Clusters with Excess ElectronS (PISCES) ,www.pisces.pitt.edu*
29. R. Antoine, P. Dugourd, D. Rayane, E. Benichou, M. Broyer, F. Chandezon and C. Guet, *J. Chem. Phys.*, 1999, **110**, 9771-9772.

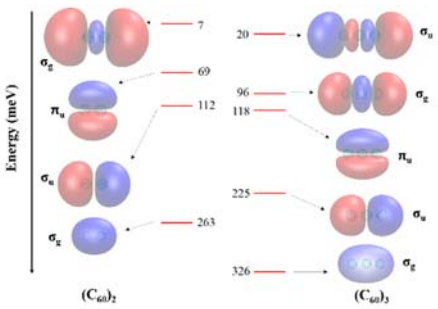

Orbitals associated with the non-valence correlation-bound anions of the C_{60} dimer and linear trimer from calculations allowing charge transfer.